Measurement of the reflectivity and absorptivity of liquids, powders, and solids at millimeter wavelengths using dielectric detection by a resonator-post fixture between parallel conducting plates

James C. Weatherall*[a], Jeffrey Barber[b], Carolyn S. Brauer, and Barry T. Smith

U.S. Department of Homeland Security, Science and Technology Directorate, Transportation Security Laboratory, Atlantic City International Airport, NJ 08405, USA;

[a]SRA International, Inc., 1201 New Road, Suite 242, Linwood, NJ 08221;

[b]Battelle Memorial Institute, 2900 Fire Road, Egg Harbor Township, NJ 08234

ABSTRACT

The appearance of a material viewed in millimeter wavelength is a function of its reflectivity and absorptivity. These optical properties can be derived from measurement of the complex dielectric constant. Knowledge of the imaginary component is particularly important to assess the brightness of transparent or semi-transparent materials, in which the return from the back surface contributes to the overall reflection. The method presented here is well-suited to determine the dielectric constant of small samples of low-loss materials, and uses a modification of the dielectric-post resonator technique in which the sample fits into a larger, solid post fixture. The measurement frequency varies only slightly among different sample materials because the electromagnetic properties of the resonance are largely set by the supporting fixture. The method can be used to measure liquids and powders, as well as solid materials. The design and electromagnetic theory of the resonant technique are described, and the precision is discussed in context of sample measurements.

Keywords: dielectric measurement, permittivity, millimeter wave, terahertz wave, explosives, imaging systems

1. INTRODUCTION

The measurement of dielectric constant is used to determine the reflection, absorption, and transmission properties of electromagnetic radiation in materials. In particular, these optical characteristics, as applied to the appropriate wave bands, determine the appearance of materials viewed in millimeter and terahertz-wave imaging systems.[1,2] While the dielectric constant governs the electromagnetic boundary conditions at material interfaces and, hence, the reflectivity, the imaginary component of the dielectric constant determines electromagnetic energy loss, and is particularly important to account for the brightness of transparent or semi-transparent materials in which the return from the back surface contributes to the overall reflection. Thus, measurement of the complex dielectric constant is important to establish electromagnetic signatures for explosive detection; it is also used to guide the development of simulants, and to establish standards for active and passive millimeter wave detection systems.[3]

The method presented here determines the dielectric constant of low-loss materials in solid, liquid, or powdered form, using a modification of the dielectric-post resonator technique (also known as the Courtney method), by which the dielectric constant of a material is measured by detecting electromagnetic resonances in a cylindrical sample of the material.[4–10] In a typical experimental setup, the sample "post" is placed between two metal plates to trap the electromagnetic modes in the cylindrical sample, but the sample is otherwise unconfined, and the excitation is done by antennas in free space. The method is desirable for measurements of explosives because it does not bring the material into direct contact with electrified probes, and the metal plates used in the system can be grounded. While the method generally uses a solid post made entirely of the material, the modification described in this paper employs a rigid, cylindrical post fixture from which a small, cylindrical column is removed; it is into this cavity that the sample material is placed.

*Email: james.weatherall@associates.dhs.gov

Sensors, and Command, Control, Communications, and Intelligence (C3I) Technologies for Homeland Security and Homeland Defense X, edited by Edward M. Carapezza, Proc. of SPIE Vol. 8019, 80190F
 · CCC code: 0277-786X/11/$18 · doi: 10.1117/12.888865

2. THE MODIFIED DIELECTRIC-POST RESONATOR

The modified post fixture consists of machined Rexolite, a low-loss plastic which has well characterized dielectric values in millimeter wavebands.[11,12] Ref 12 cites dielectric values for Rexolite at $10\,GHz$ as $\epsilon = 2.53 + 0.0011\,i$, with precision $\pm 0.02 \pm .0003\,i$. The configuration shown in Figure 1, with cavity diameter $a = 0.483\,cm$, cylinder diameter $b = 0.953\,cm$, and cylinder height $c = 0.632\,cm$, provides for the measurement in the primary TE mode at $22.6\,GHz$. Variances in the manufacture of the fixture are $\pm\,0.008\,cm$ for a, $\pm\,0.0002\,cm$ for b, and $\pm\,0.003\,cm$ for c. The cavity has an integrated floor of thickness $d = 0.0039\,cm$ to contain liquids and powders. The spatial dimensions and dielectric constant of the post are the primary determinants of the resonance frequency, so that fixtures of different sizes can access other frequencies for measurement.

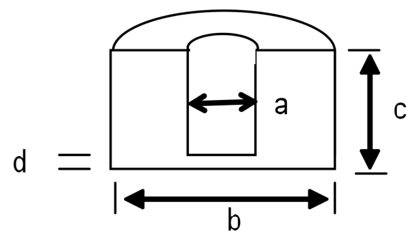

Figure 1. Cut-out view of dielectric-post resonator fixture.

The measurement system consists of the resonator post sandwiched between two parallel copper plates. The post "resonates" at frequencies where the electromagnetic field is confined to the immediate region of the post, diminishing to zero at increasing radius. Because of this asymptotic behavior, despite being $10\,cm$ in diameter, the plates are, in effect, infinite.[5] The antennas are two loop antennas entering the system through small holes in the bottom plate, with the center wire of a coax connector extending in a loop to connect on the bottom plate. The antennas are connected by $2.4\,mm$ coax to an Agilent E8364C network analyzer to measure the coupling between antennas via the S-parameter S_{21}. The frequency spectrum of the S_{21} response exhibits the resonance and the resonance width. The system is shown in Figure 2. The antennas are positioned asymmetrically relative to the resonator post, and in close proximity (at a distance of about $5\,mm$ of the outside of the fixture).

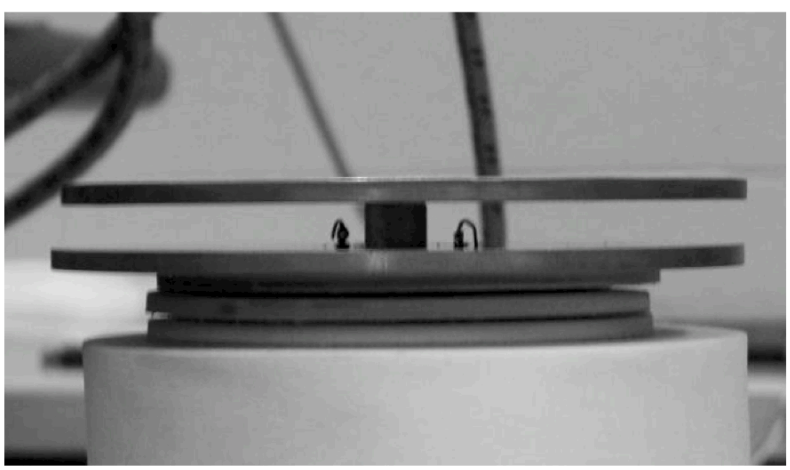

Figure 2. Dielectric-post resonator system.

The use of a fixture such as described here proves to be an effective application of this technique. In addition to providing a holder for liquids and powders, the rigid structure of the fixture provides a uniform and accurate configuration of the post, which is important for measurement precision. Another useful feature of having most of the post volume occupied by an unvarying dielectric structure is that the shift in resonance spectrum is perturbative in nature, which maintains the measurement frequency near the target value without changing the relative order or spacing of the resonances, thus making the resonance spectrum easy to interpret.

The primary advantage of this technique in characterizing the millimeter wave optical properties is that measurement of the imaginary component of the dielectric constant can be accomplished with better precision than other common methods, such as contact probes and free-space transmission/reflection methods.[13] The significance of this will be discussed further in Section 5.

Finally, the method uses relatively small amounts of material, as the sample volume is only $0.11\,ml$. This is an advantage in managing the risks associated with the measurement of sensitive materials and explosives.

3. USING THE DIELECTRIC-POST RESONATOR TO MEASURE DIELECTRIC CONSTANT

3.1 Theory of the Modal Resonance

Assuming sinusoidal time dependence $e^{-i\omega t}$ for fields in Maxwell's equations leads to Helmholtz wave equations for the electromagnetic fields $\mathbf{H}$ and $\mathbf{E}$, for which solutions are found using separation of variables in cylindrical coordinates. The boundary conditions at the conducting plates at $z = 0$ and $z = L$ require the fields E_ϕ, E_ρ, and B_z be zero; and at the dielectric boundaries at $\rho = a$ and $\rho = b$, continuity applies to normal $\mathbf{D}$ and $\mathbf{B}$, and tangential $\mathbf{E}$ and $\mathbf{H}$.

Solutions to the Helmholtz equations and boundary conditions are indexed by separation constants in the separation of variables (in the manner that modes in circular fibers are treated in Sec 8.11 of Ref. 14). In the following, solution is limited to the special case of fields that are homogeneous in ϕ-coordinate ($m = 0$ in the usual notation) and in which the trapped wave is 1/2-wavelength between the plates ($p = 1$). In the case of $m = 0$, the modes are transverse magnetic, "TM" and transverse electric "TE", where the fields everywhere have $B_z = 0$ or $E_z = 0$, respectively. (Modes with $m \neq 0$ are hybrid modes which have mixed B_z and E_z.) Among these solutions, the modes are ordered in frequency with index n. In the present dielectric-post resonator, the primary measurement mode is TE with $m = 0$, $n = 1$, and $p = 1$, and is designated TE_{011}. The TM_{011} has also been used for measurement.

Matching boundary conditions at $\rho = a$ and $\rho = b$ provides simultaneous equations which can be solved by the determinental equation

$$\begin{vmatrix} -e_1 J'(1) & 0 & e_2 J'(2) & 0 & e_2 Y'(2) & 0 & 0 & 0 \\ J(1) & 0 & -J(2) & 0 & -Y(2) & 0 & 0 & 0 \\ 0 & -u_1 J'(1) & 0 & u_2 J'(2) & 0 & u_2 Y'(2) & 0 & 0 \\ 0 & J(1) & 0 & -J(2) & 0 & -Y(2) & 0 & 0 \\ 0 & 0 & e_3 J'(3) & 0 & e_3 Y'(3) & 0 & e_4 K'(4) & 0 \\ 0 & 0 & J(3) & 0 & Y(3) & 0 & -K(4) & 0 \\ 0 & 0 & 0 & u_3 J'(3) & 0 & u_3 Y'(3) & 0 & u_4 K'(4) \\ 0 & 0 & 0 & J(3) & 0 & Y(3) & 0 & -K(4) \end{vmatrix} = 0\,. \qquad (1)$$

The notation has been simplified to make the formulation compact. Briefly, the determinant involves four limits associated with approaching the boundary at $\rho = a$ from either side, and the boundary at $\rho = b$ from either side. The notational parameters are defined in Table 1. The radial wavenumbers are given in region 1 (sample) by ${\gamma_1}^2 = \epsilon_1\,(2\pi f_0)^2/c^2 - (\pi/L)^2$, in region 2 (Rexolite fixture) by ${\gamma_2}^2 = \epsilon_2\,(2\pi f_0)^2/c^2 - (\pi/L)^2$, and in region 3 (air) by $\beta^2 = (\pi/L)^2 - (2\pi f_0)^2/c^2$, where $\epsilon_1 = \epsilon_1' + i\epsilon_1''$ and $\epsilon_2 = \epsilon_2' + i\epsilon_2''$ are the (complex) relative dielectric constants in the sample and the Rexolite region, respectively. The frequency at resonance, $f_0 = f_0' + if_0''$, will also be a complex quantity.

This formalism provides a method to derive the dielectric constant ϵ_1 from the measurement of the resonant frequency f_0. When f_0 is known by direct measurement, the unknown dielectric is found by searching for values

Table 1. Notational Definitions

region 1, $\rho = a$	*region* 2, $\rho = a$	*region* 2, $\rho = b$	*region* 3, $\rho = b$
$x_1 = \gamma_1 a$	$x_2 = \gamma_2 a$	$x_3 = \gamma_2 b$	$x_4 = \beta b$
$e_1 = \epsilon_1/x_1$	$e_2 = \epsilon_2/x_2$	$e_3 = \epsilon_2/x_3$	$e_4 = \epsilon_0/x_4$
$u_1 = 1/x_1$	$u_2 = 1/x_2$	$u_3 = 1/x_3$	$u_4 = 1/x_4$
$J(1) = J_0(x_1)$	$J(2) = J_0(x_2)$	$J(3) = J_0(x_3)$	$K(4) = K_0(x_4)$
$J'(1) = -J_1(x_1)$	$J'(2) = -J_1(x_2)$	$J'(3) = -J_1(x_3)$	$K'(4) = -K_1(x_4)$
	$Y(2) = Y_0(x_2)$	$Y(3) = Y_0(x_3)$	
	$Y'(2) = -Y_1(x_2)$	$Y'(3) = -Y_1(x_3)$	

of the dielectric which solve Equation (1). While this approach to the modal solution of the resonance equations has been very successful, electromagnetic simulation software may also be applied to identify resonances in dielectric resonators.[15]

3.2 Detection of Dielectric Constant from Measurement of Resonant Response

The TE_{011} resonance line is identified in the S_{21} spectrum by a narrow-peaked response in the vicinity of 22–23 GHz. The resonance line shape exhibits a classical damped oscillator response, and can be parameterized, with the addition of a uniform (complex) background, by:

$$S_{21} = A_0 + \frac{A_1}{f - f_0' - i\, f_0'/(2Q)}\,. \tag{2}$$

There may be a shift in resonant frequency, not included in this formulation, due to the perturbation of lossy boundary conditions;[4,14] this shift is not expected to be greater than the imaginary part of the frequency. In Equation (2), the imaginary component of the frequency is couched in terms of the Q-factor of the resonance. The imaginary component of the frequency for input into the determinental model must be corrected to exclude losses not associated with the dielectric loss, as explained next. The Lorentzian model is determined numerically from the experimental data by applying the Mathematica[16] function *FindFit* with the five fitting parameters $Re[A_0]$, $Im[A_0]$, A_1, f_0', and Q.

The detection of the dielectric constant derives from solution to Equation (1) with the input of the complex frequency $f_0' + i f_0''$. The real component is the resonance frequency as measured from the spectrum, while the

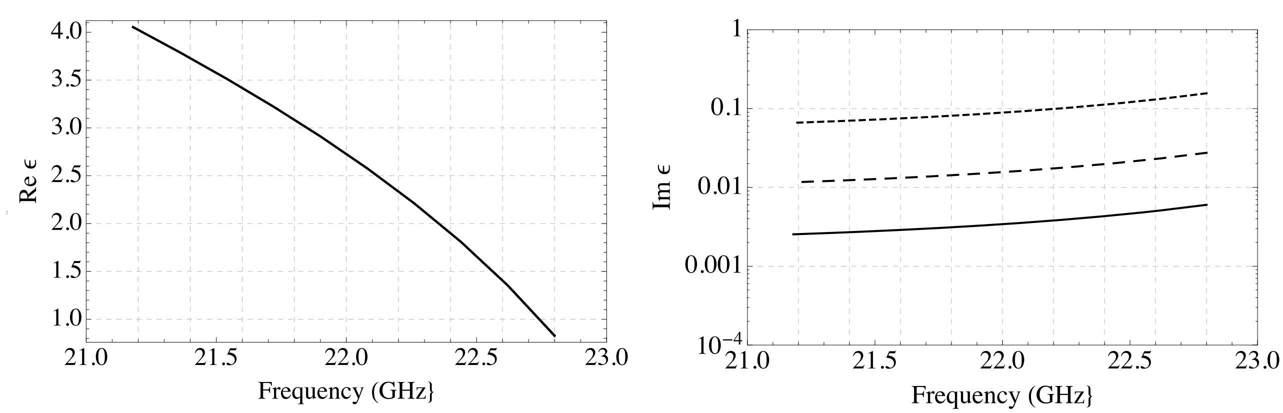

Figure 3. Dielectric as a function of frequency for three Q-factors: $Q = 1200$ (solid line), $Q = 700$ (dashed), and $Q = 200$ (dotted).

imaginary component is derived from the measurement data on the filled and empty fixtures. It is necessary to incorporate the empty fixture data because in the determinental model, the imaginary component is associated with electromagnetic energy loss which is assumed to occur entirely within the dielectric. Thus, the imaginary component of the frequency is based on what the Q-factor of the resonator would be excluding the energy loss in the Rexolite fixture, copper plates, and radiatively from the ends of the open plate system. This extraneous loss is quantified by the Q-factor of the empty fixture. The imaginary component of the frequency is thusly given by $f_0'' = f_0'/(2Q_{corr})$, where:[9]

$$\frac{1}{Q_{corr}} = \frac{1}{Q_{filled}} - \frac{1}{Q_{empty}} \,. \tag{3}$$

With the insertion of the complex frequency, the determinental condition is expressed with two equations – separating real and imaginary terms – and a numerical root finder (Mathematica[16] function *FindRoot*) is applied to solve the two equations simultaneously in unknown dielectric parameters ϵ_1' and ϵ_1'' . The dependence of the dielectric constant on the detected frequency and the detected (uncorrected) Q-factor is illustrated in Figure 3.

3.3 Measurement Precision

Variations in fixture and plate geometry occur with assembly of the resonator for measurement, and in the machining of the individual fixtures. These are expected to be primary sources of measurement error. The frequency predicted from the determinant model for the empty fixture is $22.715\,GHz$ and the Q-factor, 3300 (assuming only dielectric loss). The measurement statistics on five different fixtures are shown in Table 2.

Table 2. Statistics of Empty Fixture Measurements

Fixture	f_0	σ_f	Q_{empty}	σ_Q
*B*1	22.752	0.008	1379.	59.
*B*2	22.762	0.012	1393.	61.
*B*3	22.764	0.005	1371.	62.
*B*4	22.785	0.008	1410.	57.
*B*5	22.733	0.015	1360.	45.

On average, the standard deviation in frequency is $0.010\,GHz$ and in Q-factor is 53. These variations can be propagated into errors in the measurement of dielectric constant, for example with a Monte Carlo simulation as described in Section 4. The frequency standard deviation produces a variance in real part of the dielectric of about 3%. The expectation value for the air dielectric value is 0.95 based on the resonant-frequency mean value, so systematic errors in the dielectric are possible on the order of 0.05. For the imaginary part of the dielectric, the errors are generally smaller than 20% for $200 < Q < 1200$.

4. EXPERIMENTAL RESULTS

The focus of the material measurements is explosive materials, hazardous liquids, and various inert substances and explosive simulants. A measurement on liquid diesel fuel is presented as an example. Figure 4 shows the TE_{011} resonance data and line-fit for the fixture loaded with diesel fuel, and for comparison, the empty fixture. Using the fitted data for resonance frequency and Q-factor, the determinental equation is solved to find the sample dielectric, $\epsilon' = 2.1$ and $\epsilon'' = 0.0041$. An error analysis is performed by a Monte-Carlo simulation.[17,18] This consists of generating sets of values of f_0, Q_{filled}, and Q_{empty}, each selected randomly from distributions which have normal error distributions corresponding to the measurement means and standard deviations. For each set of values, corresponding values of dielectric constant are generated by solution of the determinental model, Equation (1). The means and standard deviations of the resulting distributions of simulated dielectric constants are evaluated. The results are shown in Figure 5. The ellipse denotes one standard deviation in measurement precision based on the propagated random error and estimated systematic error. From this analysis, the expected precision is 5% in real component and 20% in imaginary component of ϵ. This measurement of dielectric of diesel fuel is consistent with $\epsilon' = 2.19 \pm 0.05$ reported at $1.7\,GHz$ with the assumption of negligible loss.[19] It should be noted that relative to the absolute value of ϵ, the measured imaginary component is accurate to 0.03%, which is very good compared with probe measurements.[20]

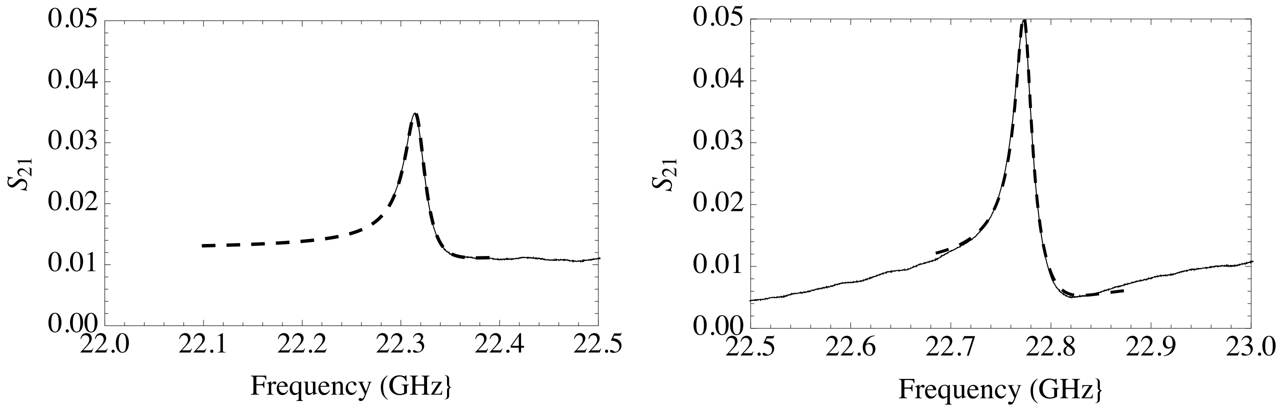

Figure 4. Resonance spectrum with diesel fuel (left) and air (right) filled fixture. Line-fitting is shown in dashed overlay. The fitted line parameters for the diesel-filled post fixture, averaged over ten measurements, are $22.305 \pm 0.015\,GHz$ and Q-factor 1123 ± 25.

5. OPTICAL PROPERTIES BASED ON DIELECTRIC MEASUREMENT

The connection between the dielectric constant measurement and the optical appearance of an object imaged in millimeter waves is made through geometric optics. Consider a plane wave which is described as the real part of the complex quantity

$$E(x,t) = \mathcal{E} e^{ikx - iwt} \,. \tag{4}$$

In a dielectric medium, the wavenumber k of an electromagnetic wave is related to its frequency $\omega = 2\pi f$ by

$$kc = \sqrt{\mu\epsilon}\,\omega \,, \tag{5}$$

where μ and ϵ are permeability and permittivity relative to empty space. Thus, when the dielectric is a complex number, the wavevector is also complex. Assuming $\mu = 1$, and writing $n = \sqrt{\epsilon} = n' + i\,n''$ (here n is the complex index of refraction), the plane-wave electric field is the real part of the complex quantity

$$E(x,t) = \mathcal{E} e^{-n''(\omega/c)x}\, e^{in'(\omega/c)x - i\omega t} \,. \tag{6}$$

The reflection and transmission of electromagnetic waves at a plane interface can be described using conventional Fresnel formulas using the (complex) refractive index; transmission losses in the medium can be described according to the exponential term in Equation (6).

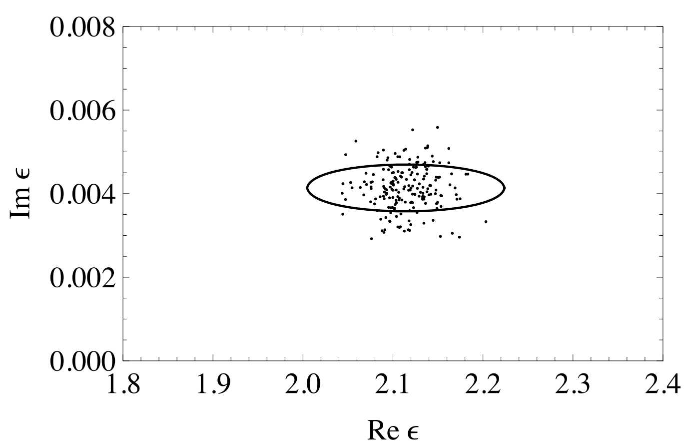

Figure 5. Distribution of diesel fuel dielectric values in a Monte-Carlo simulation based on measurement and statistics. The ellipse denotes the measurement precision.

Because objects being imaged in millimeter waves are often on the order of a wavelength in thickness, the total reflected field may involve multiple reflections from front and back surfaces. To account for intensity of radiation reflected from an object, accurate knowledge of the optical properties (refractive index) is necessary. When the illumination bandwidth is sufficiently narrow, the oscillatory term involving n' in Eq. (6) determines how multiple reflections will add together, in or out of phase. Also, for material depths x for which the magnitude of the exponent in the n''-term is greater than unity, transmission losses allow only the reflection from the front surface to be observed. These issues in how radiation interacts with materials are important for characterizing detection signatures, and in identifying explosive simulant materials.[3]

6. CONCLUSION

The use of a modified dielectric-post resonator technique to measure dielectric constant at 21–23 GHz is demonstrated. The technique is used on liquid, powdered, and solid samples, with volume on the order of $0.10\,ml$. The measurement of the imaginary component of the dielectric constant is generally decoupled from the measurement of the real component, so one of the main advantages to this measurement system is that precise measurements can be made on low loss materials which have small imaginary components. The technique appears to be most useful for low loss materials with imaginary component of dielectric between 0.002 and 0.2. The main limitations are due to the Q-factor of the unloaded fixture, and the difficulty in detecting broad resonances from instrumental background noise.[10]

The primary resonant mode for measurement has been the lowest frequency TE mode, TE_{011}. Additional modes which have been identified[8] include the HE_{111} mode at $19\,GHz$ and the TM_{011} mode at $23\,GHz$. Application of this method to these modes would provide additional data points, or possible information about frequency dispersion.

ACKNOWLEDGMENTS

This work was supported by DHS contract HSHQDC09-F-00043. C.S.B. was supported in part by an appointment to the TSL Visiting Scientist Program administered by the Oak Ridge Institute for Science and Education through an interagency agreement between the U.S. Department of Energy and the U.S. Department of Homeland Security. ORISE is managed by Oak Ridge Associated Universities (ORAU) under DOE contract number DE-AC05-06OR23100.

REFERENCES

[1] Salmon, N. A., "Polarimetric scene simulation in millimeter-wave radiometric imaging," *Radar Sensor Technology VIII and Passive Millimeter-Wave Imaging Technology VII, Proc. SPIE* **5410**, 260–269 (2004).

[2] Weatherall, J. C., "Emission from dielectric materials at millimeter wavelengths in passive thermal environments," *Passive Millimeter-Wave Imaging Technology XIII* **7670**(1), 76700F, SPIE (2010).

[3] Barber, J., Weatherall, J. C., Smith, B. T., Duffy, S., Goettler, S. J., and Krauss, R. A., "Millimeter wave measurements of explosives and simulants," *Passive Millimeter-Wave Imaging Technology XIII* **7670**(1), 76700E, SPIE (2010).

[4] Hakki, B. and Coleman, P., "A dielectric resonator method of measuring inductive capacities in the millimeter range," *IRE Transactions on Microwave Theory and Techniques* **8**(4), 402–410 (1960).

[5] Courtney, W., "Analysis and evaluation of a method of measuring the complex permittivity and permeability of microwave insulators," *Microwave Theory and Techniques, IEEE Transactions on* **18**(8), 476–485 (1970).

[6] Kobayashi, Y. and Tanaka, S., "Resonant modes of a dielectric rod resonator short-circuited at both ends by parallel conducting plates," *IEEE Transactions on Microwave Theory and Techniques* **MTT-28**(10), 1077–1085 (1980).

[7] Kobayashi, Y. and Katoh, M., "Microwave measurement of dielectric properties of low-loss materials by the dielectric rod resonator method," *IEEE Transactions on Microwave Theory and Techniques* **33**(7), 586–592 (1985).

[8] Wheless, P. and Kajfez, D., "The use of higher resonant modes in measuring the dielectric constant of dielectric resonators," in [*Microwave Symposium Digest, 1985 IEEE MTT-S International*], 473–476 (1985).

[9] Gershon, D., Calame, J., Carmel, Y., and Antonsen, T., "Adjustable resonant cavity for measuring the complex permittivity of dielectric materials," *Review of Scientific Instruments* **71**(8), 3207–3209 (2000).

[10] Nedelcu, L., Toacsan, M., Banciu, M., and Ioachim, A., "Dielectric resonators for microwave and millimeter wave applications," in [*Semiconductor Conference, 2007. CAS 2007. International*], **1**, 275–278 (2007).

[11] Meriakri, V. and Fernandes, C., "Materials for application in millimeter and submillimeter ranges," in [*Microwave and Optoelectronics Conference, 1999. SBMO/IEEE MIT-S, APS and LEOS - IMOC '99 International*], 532–534 vol. 2 (1999).

[12] Baker-Jarvis, J., Janezic, M. D., Riddle, B. F., and Holloway, C. L., "Dielectric and conductor-loss characterization and measurements on electronic packaging materials," Tech. Rep. 1520, National Institute of Standards and Technology (2001).

[13] Baker-Jarvis, J., Janezic, M. D., Riddle, B. F., Johnk, R. T., Kabos, P., and Holloway, C. L., "Measuring the permittivity and permeability of lossy materials: Solids, liquids, metals, building materials, and negative-index materials," Tech. Rep. 1536, National Institute of Standards and Technology (2005).

[14] Jackson, J. D., [*Classical Electrodynamics*], John Wiley & Sons, New York, third ed. (1998).

[15] Lui, M.-L. and Wu, K.-L., "An efficient integral equation analysis for characterizing lossy dielectric resonator," in [*Microwave Symposium Digest, 2004 IEEE MTT-S International*], **3**, 1835–1838 (2004).

[16] Wolfram Research, [*Mathematica*], Wolfram Research, Inc., Champaign, Illinois, version 8.0 ed. (2010).

[17] Morgan, M. and Henrion, M., [*Uncertainty: A Guide to Dealing with Uncertainty in Quantitative Risk and Policy Analysis*], Cambridge University Press (1990). Chapter 8.

[18] Metropolis, N., "The beginning of the Monte Carlo method," *Los Alamos Science* **15**, 125–130 (1987). 1987 Special Issue Dedicated to Stanislaw Ulam.

[19] Cataldo, A., Torricone, L., Vallone, M., Attivissimo, F., and Trotta, A., "An assessment of the accuracy of time-domain reflectometry for measuring level and permittivity of liquids," in [*Instrumentation and Measurement Technology Conference, 2006. IMTC 2006. Proceedings of the IEEE*], 2332–2337 (2006).

[20] Agilent Technologies, Inc., "Agilent 85070E dielectric probe kit 200 MHz to 50 GHz: Technical overview." www.agilent.com (2008).